Photoemission study of carriers and Ce 4f spectral weight in CeTe$_2$

INSTITUTE OF PHYSICS PUBLISHING

JOURNAL OF PHYSICS: CONDENSED MATTER

J. Phys.: Condens. Matter **16** (2004) 9163–9168

PII: S0953-8984(04)85740-0

Photoemission study of carriers and Ce 4f spectral weight in CeTe$_2$

J-S Kang[1,4]**, C G Olson**[2]**, Y S Kwon**[3,4]**, S W Han**[2]**, K H Kim**[5]**, A Sekiyama**[6]**, S Kasai**[6]**, S Suga**[6]** and B I Min**[7]

[1] Department of Physics, The Catholic University of Korea, Puchon 420-743, Korea
[2] Ames Laboratory, Iowa State University, Ames, IA 50011, USA
[3] Department of Physics, Sungkyunkwan University, Suwon 440-746, Korea
[4] CSCMR, Seoul National University, Seoul 151-742, Korea
[5] Department of Physics, Gyeongsang National University, Chinju 660-701, Korea
[6] Department of Material Physics, Graduate School of Engineering Science, Osaka University, Osaka 560-8531, Japan
[7] Department of Physics, Pohang University of Science and Technology, Pohang 790-784, Korea

Abstract

The electronic structure of CeTe$_2$ has been investigated by performing high-resolution photoemission spectroscopy (PES) measurements on high-quality stoichiometric single crystals of CeTe$_2$. The Ce 3d XAS measurement indicates that the Ce ions are trivalent. The Ce 4f PES spectrum reveals two-peak structures with the Ce 4f *bulk* hybridization peak located around 0.8 eV below E_F. The high-resolution, high-energy, *bulk*-sensitive PES study of CeTe$_2$ provides evidence for a metallic density of states near E_F. The carriers near E_F consist mainly of Ce 5d and Te(1) 5p states, while the contribution from the Ce 4f and Te(2) 5p states is negligible. This finding agrees with the CDW instability in the Te(1) sheets.

Layered RTe$_2$ (R: La, Ce) systems have attracted much attention due to their anomalous magnetic and transport properties. RTe$_2$ crystallizes in the layered Cu$_2$Sb-type tetragonal structure with two types of Te sites: Te(1) and Te(2). Te(1) atoms form the planar square sheet which is sandwiched by the corrugated double layers formed of R and Te(2) atoms. LaTe$_2$ exhibits the charge density wave (CDW) instability in the Te(1) square sheets [1–4]. CeTe$_2$ also shows the CDW-related pseudo-gap feature [4] and the superstructure [5]. Due to the quasi-two-dimensional layered structure, CeTe$_2$ shows strong anisotropic behaviour in transport and magnetic properties [6–9].

In order to understand the origin of the anomalous magnetic and transport properties of CeTe$_2$, it is essential to investigate the electronic structure of CeTe$_2$ and the role of Ce 4f electrons. One of the open issues in CeTe$_2$ is the nature of the charge carriers: it

is not clear whether they come from Te(1), Te(2), or Ce. It is generally considered that the ionic configuration of RTe_2 is $R^{3+}Te(2)^{2-}Te(1)^{1-}$ so as to produce hole carriers in the Te(1) sheets. This idea, however, has not been confirmed experimentally. Most of previous experiments were done on non-stoichiometric samples with a Te deficiency because of the difficulty in growing high-quality stoichiometric single crystals [6, 7]. Due to the extremely low carrier concentration in $CeTe_2$, non-stoichiometry affects the physical properties a lot. Only a few electronic structure studies have been reported for RTe_2. Break junction tunnelling measurements on polycrystalline samples [4] showed that $LaTe_2$ has a well-developed CDW gap (2Δ) of 0.9 eV, whereas $CeTe_2$ has a V-shaped density of states (DOS) near the Fermi level E_F with the in-gap states. The ultraviolet photoemission spectroscopy (PES) study on a polycrystalline $LaTe_2$ sample [10] was consistent with a very low carrier density at E_F.

In this study, we report a high-resolution PES study on stoichiometric single crystals of RTe_2 (R = Ce, La). We have determined the partial spectral weight (PSW) distributions of the *bulk* Ce 4f, La 5d, and Te p electrons, and the type of the carriers in $CeTe_2$, by performing resonant PES (RPES) measurements near the La and Ce 3d $\rightarrow$ 4f absorption edges.

RTe_2 single crystals (R = La, Ce) were grown by the self-fluxed Bridgman method [7]. Electron-probe microanalysis (EPMA) of several parts of the samples showed that the atomic ratios of R to Te were Ce:Te = 1:2.00 $\pm$ 0.02 and La:Te = 1:1.99 $\pm$ 0.02. The residual resistivity of these samples is a few hundred times smaller than that of previously reported samples [7].

High-resolution Ce 3d $\rightarrow$ 4f RPES experiments were performed at the twin-helical undulator beam-line BL25SU of SPring-8 equipped with a SCIENTA SES200 analyser. Samples were cleaved and measured in vacuum better than 3×10^{-10} Torr at $T \lesssim 20$ K. PES data were obtained in the transmission mode. The total instrumental resolution (FWHM: full width at half maximum) of the system was about 100 meV at $h\nu \sim 880$ eV. All the spectra were normalized to the incident photon flux. The cleanliness of the cleaved surfaces was confirmed by the absence of the O 1s peak. XAS spectra were obtained by employing the total electron yield method, with the photon energy resolution better than ~ 100 meV at $h\nu \approx 900$ eV.

Ce 4d $\rightarrow$ 4f RPES experiments were carried out at the PGM beam-line at the Synchrotron Radiation Center (SRC). Samples were cooled down to $T \lesssim 15$ K and cleaved in vacuum with a base pressure better than 3×10^{-11} Torr. The cleanliness of the cleaved surfaces was confirmed by the absence of the 6 eV peak and no hump at about 9.5 eV [11]. The Fermi level and the overall instrumental resolution of the system were determined from the valence-band spectrum of a sputtered Pt foil. The FWHM was about 160 meV at $h\nu \sim 120$ eV.

Figure 1 shows the R 3d XAS spectra of RTe_2 (R = Ce, La). The Ce 3d XAS spectrum of $CeTe_2$ is very similar to that of a trivalent (3+) Ce compound CeNiSn [12], but different from those of the mixed-valent Ce compounds $CeNi_x$ ($x = 2, 5$) [13] and a formally tetravalent (4+) CeO_2 [14]. The main peaks in the Ce $3d_{5/2}$ XAS part ($h\nu \approx 881.4$ and 882.4 eV) and the shoulder structures at lower $h\nu$ ($h\nu \sim 878$–880 eV) are ascribed to multiplet structures due to the $3d^{10}4f^1 \rightarrow 3d^9 4f^2$ transition. Further, no satellite structure is observed near $h\nu \sim 887$ eV, corresponding to the $3d^{10}4f^0 \rightarrow 3d^9 4f^1$ transition, indicating that there is almost no $3d^{10}4f^0$ configuration in the ground state of $CeTe_2$. These features indicate that the ground states of Ce ions in $CeTe_2$ are nearly trivalent with the $|g\rangle \approx 3d^{10}4f^1$ configuration. The La 3d XAS spectrum of $LaTe_2$ is very similar to that of a formally trivalent (3+) La oxide La_2O_3 [14], which has the $4f^0$ configuration in the ground state. Figure 1 thus indicates that the valence states of *bulk* Ce and La ions in RTe_2 are mainly trivalent (3+) states.

Figure 2 compares two different results of the extracted Ce 4f PSW distributions of $CeTe_2$. These methods used the traditional giant resonances in Ce 3d $\rightarrow$ 4f RPES [12] and Ce 4d $\rightarrow$ 4f
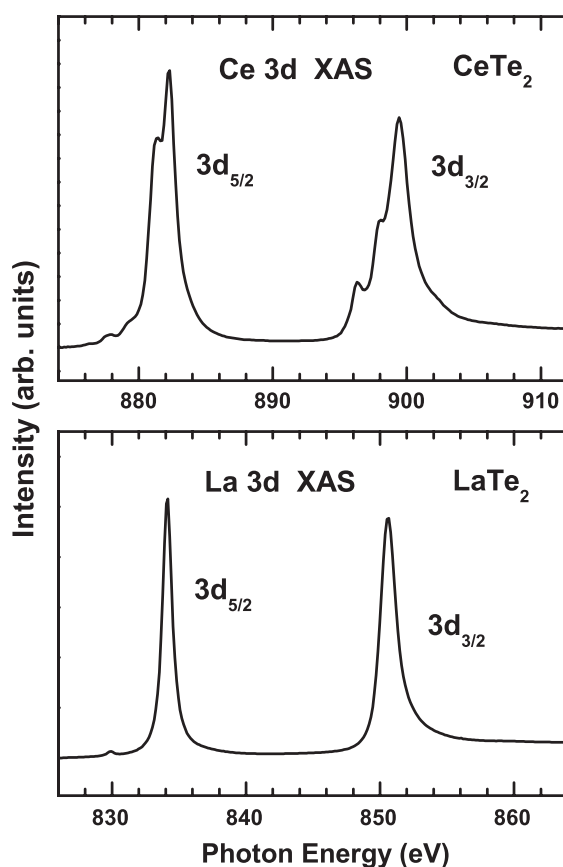
Figure 1. The Ce 3d XAS spectrum of CeTe$_2$ (top) and the La 3d XAS spectrum of LaTe$_2$ (bottom).

RPES [15], respectively, and the standard extraction procedure. $h\nu \approx 874.8$ and 882.4 eV were employed in 3d $\rightarrow$ 4f RPES (solid curves) and $h\nu \approx 115$ and 121 eV were employed in 4d $\rightarrow$ 4f RPES (open circles). The resonance enhancement identifies the features as having 4f character.

Both Ce 4f PSWs show two-peak structures, with the lower binding energy peak around 0.8–1.2 eV, and the higher binding energy peak around 4 eV. The two-peak structures are typical of Ce compounds, but the lower binding energy peak in CeTe$_2$ is located far below E_F without a Kondo resonance near E_F [16][8]. The high and low binding energy peaks are identified as due to the $4f^1 v^m \rightarrow 4f^0 v^m$ and $4f^1 v^m \rightarrow 4f^1 v^{m-1}$ transitions (v denotes a valence-band electron), respectively [15]. The low binding energy peak arises from the hybridization between the Ce 4f and valence-band electrons [15, 17].

It is well known that the Ce 4f spectrum determined from Ce 3d $\rightarrow$ 4f RPES is more representative of the *bulk* Ce 4f spectrum, [18, 19] as compared to Ce 4d $\rightarrow$ 4f RPES, which contains a large contribution from the *surface* emission. It is found that the *bulk* Ce 4f hybridization peak of CeTe$_2$ is located around 0.8 eV binding energy, and the peak

---

[8] The absence of the Kondo resonance in CeTe$_2$ is due to the very low conduction electron concentration in CeTe$_2$ since the Kondo resonance can be observed only in metallic systems.
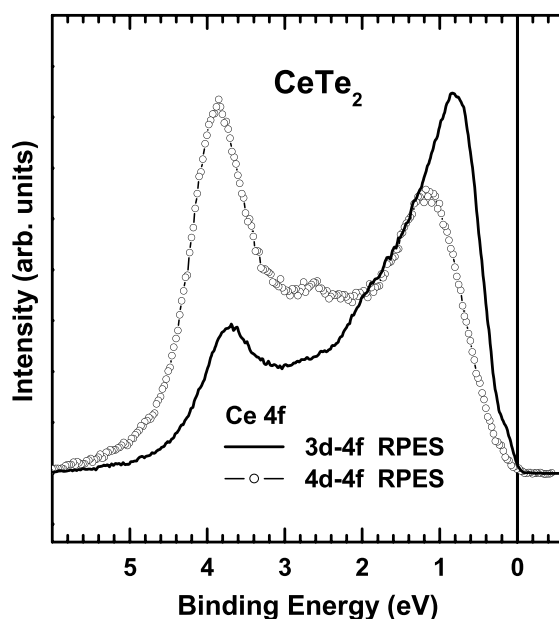
Figure 2. Comparison of the Ce 4f PSWs of CeTe$_2$, determined from Ce 3d $\rightarrow$ 4f RPES, and Ce 4d $\rightarrow$ 4f RPES. All the data were obtained at normal emission.

is rather broad, corresponding to FWHM $\sim$ 1.5 eV. The broad 4f bands indicate large hybridization between Ce 4f and Te 5p electrons. The comparison in figure 2 shows that the Ce 4f hybridization peak in the *surface*-sensitive Ce 4f PSW is at a higher binding energy ($\sim$1.2 eV) than the *bulk* peak ($\sim$0.8 eV). Further, the Ce 4f intensity near E_F in the *bulk*-sensitive Ce 4f PSW is much larger than that in the *surface*-sensitive Ce 4f PSW. Note, however, that the contribution from the Ce 4f states just at E_F is negligible. In other words, there are no metallic Ce 4f states at E_F, but the Ce 4f states are located slightly below E_F. This point will be discussed further in figure 3.

Figure 3 shows the extracted PSW distributions in CeTe$_2$ for different orbitals. The top curve of the Ce 4f PSW corresponds to that determined from the 3d $\rightarrow$ 4f RPES, shown in figure 2. Even in using high $h\nu$ in Ce 3d $\rightarrow$ 4f RPES [18, 19], one should be cautious in determining the *bulk* Ce 4f PSW, due to the *surface* 4f emission and the resonant Ce 5d emission. As shown in figure 2, most of the *surface* contribution is likely to be underneath the high-energy peak around $\sim$4 eV. As for the resonant Ce 5d intensity in the Ce 4f PSW, the contribution is estimated to be less than 10% [20]. As mentioned above, the contribution from the Ce 4f states at E_F is negligible even though there is a small hump below E_F.

As to the Ce 5d PSW, we consider the Ce 5d PSW to be similar to the La 5d PSW to a first approximation. It is very difficult to extract the Ce 5d emission due to the overlap with the stronger Ce 4f emission. We have determined the La/Ce 5d PSW by using the standard extraction procedure in the La 5d resonance in La 3d $\rightarrow$ 4f RPES, where $h\nu \approx 834$ and 828 eV are used as the on- and off-resonance energies, respectively. The La/Ce 5d PSW of RTe$_2$ clearly exhibits a metallic Fermi edge.

The off-resonance spectrum ($h\nu \approx 828$ eV) in La 3d $\rightarrow$ 4f RPES is chosen to represent the Te 5p PSW because the Te 5p emission is dominant over other electron emissions around this $h\nu$ value [21]. Note that the intensity near E_F is non-negligible in the PES spectrum with $h\nu \approx 828$ eV. The $h\nu \approx 828$ eV spectrum that represents the *bulk* Te 5p PSW consists of both
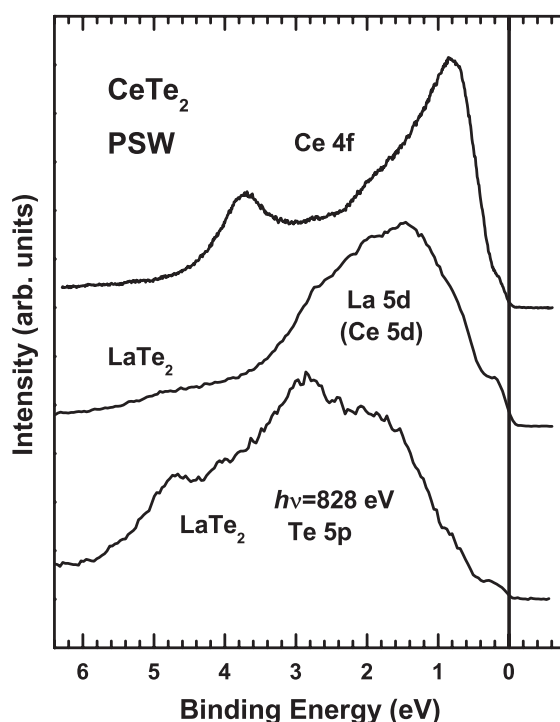
Figure 3. The extracted PSW distributions for CeTe$_2$ for different orbitals. The Ce 5d PSW for CeTe$_2$ is assumed to be similar to the La 5d PSW for LaTe$_2$. All the data were obtained at the normal emission, and the vertical scale is arbitrary for each spectrum.

Te(1) and Te(2) 5p electron emissions. This feature of non-negligible Te 5p states near E_F is quite different from the gap feature observed in the *surface*-sensitive tunnelling spectrum [4]. The calculated band structure of the CDW phase of LaTe$_2$ shows that [5] the Te(2) 5p bands lie far below E_F, whereas the Te(1) 5p bands are close to E_F. Thus the tunnelling spectrum seems to represent the DOS mainly from the R–Te(2) planes. Accordingly, the non-negligible intensity near E_F at $h\nu \approx 828$ eV, as compared to the gap feature in the tunnelling spectrum, implies that the Te(1) 5p states are located still closer to E_F than the Te(2) 5p states, despite the CDW gap opening in the Te(1) sheets in CeTe$_2$. Our PES data indicate that the CDW gap in the Te(1) sheets is much smaller than the value reported from the tunnelling experiment [4] ($2\Delta = 0.9$ eV for LaTe$_2$). Therefore our high-resolution PES data for CeTe$_2$ are consistent with the existence of the Te(1) 5p electronic states near E_F, as predicted in the band calculation [3].

The metallic Fermi edge is clearly observed only in the La/Ce 5d PSW, but not in Te 5p and Ce 4f PSWs, reflecting that only the Ce 5d bands cross E_F. Therefore this finding implies that, in CeTe$_2$, the electronic states near E_F have little Ce 4f character, so that the carriers near E_F have mainly Ce 5d character. This conclusion is consistent with the metallic ground states of LaTe$_2$ and CeTe$_2$ [7], and also with the picture of the CDW instability in the Te(1) sheets. According to band-theoretical calculations [3], the La 5d states are shifted down to cut E_F when the lattice distortion due to the CDW instability in the Te(1) sheets is taken into account.

In conclusion, the Ce 4f PSW of CeTe$_2$ has been determined by employing *bulk*-sensitive 3d → 4f RPES and XAS. Among the two-peak structures of the Ce 4f PSW for CeTe$_2$, the position of the Ce 4f *bulk* hybridization peak is located around 0.8 eV binding energy. The

Ce and La 3d XAS spectra show trivalent (3+) *bulk* Ce and La ions in $CeTe_2$ and $LaTe_2$. In the high-resolution *bulk*-sensitive PES spectra for RTe_2, the metallic Fermi edge is observed only in the La/Ce 5d PSW, but not in the Te 5p and Ce 4f PSWs, reflecting that only the Ce 5d bands cross E_F. Our high-resolution PES spectra near E_F also indicate that the Te(1) 5p bands are located much closer to E_F than the Te(2) 5p bands. Therefore this PES study for $CeTe_2$ suggests that the Ce 5d and Te(1) 5p electrons, located near E_F, play an important role in determining the metallic ground state of $CeTe_2$. Our finding is consistent with the CDW instability in the Te(1) sheets.

Acknowledgments

References

[1] DiMasi E, Foran B, Aronson M C and Lee S 1996 *Phys. Rev.* B **54** 13587
[2] Kikuchi A 1998 *J. Phys. Soc. Japan* **67** 1308
[3] Stöwe K 2000 *J. Solid State Chem.* **149** 155
[4] Jung M H, Ekino T, Kwon Y S and Takabatake T 2001 *Phys. Rev.* B **63** 035101
[5] Stöwe K 2000 *J. Alloys Compounds* **307** 101
[6] Min B H, Choi H Y and Kwon Y S 2002 *Physica* B **312/313** 203
[7] Min B H, Moon E D, Im H J, Hong S O, Kwon Y S, Kim D L and Ri H C 2002 *Physica* B **312/313** 205
[8] Jung M H, Min B H, Kwon Y S, Oguro I, Iga F, Fujita T, Ekino T, Kasuya T and Takabatake T 2000 *J. Phys. Soc. Japan* **69** 937
[9] Kasuya T, Jung M-H and Takabatake T 2000 *J. Magn. Magn. Mater.* **220** 235
[10] Chung J, Park J H, Park J-G, Choi B-H, Oh S-J, Cho E-J, Kim H-D and Kwon Y S 2001 *J. Korean Phys. Soc.* **38** 744
[11] Kang J-S, Olson C G, Jung J H, Lee S T, Noh T W and Min B I 1999 *Phys. Rev.* B **60** 13257
[12] Sekiyama A, Suga S, Iwasaki T, Ueda S, Imada S, Saitoh Y, Yoshino T, Adroja D T and Takabatake T 2001 *J. Electron Spectrosc. Relat. Phenom.* **114–116** 699
[13] Jung R-J, Choi B-H, Oh S-J, Kim H-D, Cho E-J, Iwasaki T, Sekiyama A, Imada S, Suga S and Park J-G 2003 *Phys. Rev. Lett.* **91** 157601
[14] Han S W, Kang J-S, Kim K H, Lee J D, Kim J H, Wi S C, Mitra C, Raychaudhyri P, Wirth S, Kim K J, Kim B S, Jeong J I, Kwon S K and Min B I 2004 *Phys. Rev.* B **69** 104406
[15] Allen J W, Oh S-J, Gunnarsson O, Schönhammer K, Maple M B, Torikachvili M S and Lindau I 1987 *Adv. Phys.* **35** 275
[16] Gunnarsson O and Schönhammer K 1983 *Phys. Rev.* B **28** 4315
[17] Min B I, Jansen H J F, Oguchi T and Freeman A J 1986 *Phys. Rev.* B **33** 8005
[18] Duo L 1998 *Surf. Sci. Rep.* **32** 233
[19] Sekiyama A, Iwasaki T, Matsuda K, Saitoh Y, Onuki Y and Suga S 2000 *Nature* **403** 398
[20] Kang J-S 2004 unpublished data
[21] Yeh J J and Lindau I 1985 *At. Data Nucl. Data Tables* **32** 1